Published in final edited form as:
J Neurosurg. 2011 July ; 115(1): 11–17. doi:10.3171/2011.2.JNS101451.

Quantitative fluorescence in intracranial tumor: implications for ALA-induced PpIX as an intraoperative biomarker

Pablo A. Valdés, B.S.[1,2], **Frederic Leblond, Ph.D.**[1], **Anthony Kim, Ph.D.**[3], **Brent T. Harris, M.D., Ph.D.**[2,5], **Brian C. Wilson, Ph.D.**[3], **Xiaoyao Fan, B.E.**[1], **Tor D. Tosteson, Sc.D.**[2,4], **Alex Hartov, Ph.D.**[1], **Songbai Ji, D.Sc.**[1], **Kadir Erkmen, M.D.**[2,6], **Nathan E. Simmons, M.D.**[2,6], **Keith D. Paulsen, Ph.D.**[1,4], and **David W. Roberts, M.D.**[2,4,6]

[1]Thayer School of Engineering, Dartmouth College, Hanover

[2]Dartmouth Medical School, Dartmouth College, Hanover

[3]University of Toronto, Ontario Cancer Institute/University Health Network, Toronto, Ontario, Canada

[4]Norris Cotton Cancer Center, Dartmouth-Hitchcock Medical Center, Lebanon, New Hampshire

[5]Department of Pathology, Dartmouth-Hitchcock Medical Center, Lebanon, New Hampshire

[6]Section of Neurosurgery, Dartmouth-Hitchcock Medical Center, Lebanon, New Hampshire

Abstract

Object—Accurate discrimination between tumor and normal tissue is crucial for optimal tumor resection. Qualitative fluorescence of protoporphyrin IX (PpIX), synthesized endogenously following δ-aminolevulinic acid (ALA) administration, has been used for this purpose in high-grade glioma (HGG). The authors show that diagnostically significant but visually imperceptible concentrations of PpIX can be quantitatively measured in vivo and used to discriminate normal from neoplastic brain tissue across a range of tumor histologies.

Methods—The authors studied 14 patients with diagnoses of low-grade glioma (LGG), HGG, meningioma, and metastasis under an institutional review board–approved protocol for fluorescence-guided resection. The primary aim of the study was to compare the diagnostic capabilities of a highly sensitive, spectrally resolved quantitative fluorescence approach to conventional fluorescence imaging for detection of neoplastic tissue in vivo.

Results—A significant difference in the quantitative measurements of PpIX concentration occurred in all tumor groups compared with normal brain tissue. Receiver operating characteristic (ROC) curve analysis of PpIX concentration as a diagnostic variable for detection of neoplastic tissue yielded a classification efficiency of 87% (AUC = 0.95, specificity = 92%, sensitivity = 84%) compared with 66% (AUC = 0.73, specificity = 100%, sensitivity = 47%) for conventional fluorescence imaging ($p < 0.0001$). More than 81% (57 of 70) of the quantitative fluorescence

Address correspondence to: David W. Roberts, M.D., Section of Neurosurgery, Dartmouth-Hitchcock Medical Center, One Medical Center Drive, Lebanon, New Hampshire 03756. David.W.Roberts@dartmouth.edu.

Portions of this work were presented at the Optical Society of America Conference, Miami, Florida, April 2010.

Author contributions to the study and manuscript preparation include the following. Conception and design: Roberts, Valdes, Leblond, Kim, Harris, Wilson, Paulsen. Acquisition of data: Roberts, Valdes, Fan, Hartov, Ji, Erkmen, Simmons. Analysis and interpretation of data: Roberts, Valdes, Leblond, Harris. Drafting the article: Valdes, Leblond, Paulsen. Critically revising the article: Roberts, Valdes, Leblond, Kim, Harris, Wilson, Tosteson, Paulsen. Reviewed final version of the manuscript and approved it for submission: all authors. Statistical analysis: Valdes, Tosteson. Administrative/technical/material support: Fan, Hartov, Ji. Study supervision: Roberts, Leblond, Paulsen. Developed quantitative fluorescence system: Kim, Wilson. Evaluated histopathology: Harris.

measurements that were below the threshold of the surgeon's visual perception were classified correctly in an analysis of all tumors.

Conclusions—These findings are clinically profound because they demonstrate that ALA-induced PpIX is a targeting biomarker for a variety of intracranial tumors beyond HGGs. This study is the first to measure quantitative ALA-induced PpIX concentrations in vivo, and the results have broad implications for guidance during resection of intracranial tumors.

Keywords

ALA; PpIX; biophotonics; brain tumor; fluorescence-guided resection; optical spectroscopy; oncology; light-transport modeling; glioma

---

Biomarkers that are specific to malignancies and can be imaged or otherwise detected during intraoperative procedures hold significant promise in the treatment and management of disease.[22] Indeed, several clinical studies have shown that HGGs accumulate the endogenous fluorescent biomarker, PpIX, specifically and in concentrations sufficient for visual detection during surgery under blue light exposure after exogenous administration of ALA.[4,8–10,14,17,18,21,23] The net effect has been the realization of a tumor-specific biomarker for surgical guidance that has improved completeness of resection of HGGs and has led to statistically significant increases in progression-free survival in this patient population in a randomized, controlled Phase III clinical trial.[9,18,19] Unfortunately, the same has not been true for lower-grade disease in which the clinical impact in terms of prolonging survival could be more substantial.[17,23] Here, we show for the first time that concentrations of PpIX exist in intracranial tumors that are below the threshold of human visual perception and that this biomarker, when detected quantitatively, offers classification efficiencies of up to 97% with corresponding sensitivities and specificities greater than 90%, which far exceed the diagnostic performance of the human eye and current fluorescence imaging technologies.

Methods

Patient Selection

The institutional review board governing the participation of humans in research at Dartmouth-Hitchcock Medical Center approved our fluorescence-guided intracranial tumor resection protocol. All patients participated under informed consent. Inclusion criteria were preoperative diagnosis of LGG, HGG, meningioma, or metastatic brain tumor; tumor judged suitable for open cranial resection; age equal to or older than 18 years; and patient ability to provide informed consent. Exclusion criteria included pregnancy or breast feeding; history of cutaneous photosensitivity or hypersensitivity to porphyrins; photodermatosis, exfoliative dermatitis, or porphyria; history of liver disease within the last 12 months; alanine aminotransferase, aspartate aminotransferase, alkaline phosphatase, or bilirubin levels greater than 2.5 times the normal limit at any time during the previous 2 months; plasma creatinine in excess of 180 μmol/L; patient inability to comply with the photosensitivity precautions associated with the study; and serious associated psychiatric illness. Patients were given an oral dose (20 mg/kg body weight) of ALA (DUSA Pharmaceuticals) dissolved in 100 ml of water approximately 3 hours prior to the induction of anesthesia. Preoperative, high-resolution contrast-enhanced T1- and/or T2-weighted axial images were acquired and used for navigational guidance.

Intraoperative Probe

We used a fiberoptic probe connected to a spectrometer to measure the response of brain tissue excited with blue light (wavelength: $\lambda = 405$ nm) followed by interrogation with broadband white light ($\lambda = 450–720$ nm) delivered through the fiberoptic probe tip to

compensate for signal losses due to light absorption and scattering by the tissue using novel light-transport modeling methods.[7] The relative contributions of oxyhemoglobin and deoxyhemoglobin to the total light absorption were determined in situ by using the measured white-light reflectance spectrum fitted to a diffusion model of the reflectance where the intrinsic absorption spectra of each of these proteins were assumed to be known.

A mathematical model[7] (Appendix) was then used to quantify the absolute concentration of PpIX based on the measured fluorescence spectrum. Since the fluorescence measurements are distorted by variations in tissue optical properties, quantitative determination of the concentration of fluorescing molecules requires knowledge of the absorption and scattering spectra of the tissue being sampled. Moreover, PpIX is not the only molecule contributing to the measured fluorescence spectrum (other contributors include tissue autofluorescence and photoproducts such as photoprotoporphyrin resulting from PpIX photobleaching[3]). However, the spectral shapes of the primary fluorophores of interest are known, which allows spectral decomposition to be used to determine their relative contributions, and in the case of PpIX, the absolute concentration (C_{PpIX}). By incorporating these light-transport modeling methods that eliminate the distorting effects of variations in tissue optical properties and account for the presence of multiple fluorescent species, quantitative measurements of C_{PpIX} can be obtained intraoperatively and in vivo with an unprecedented degree of sensitivity and fidelity.

Surgical Procedure

The patient's head was prepared and registered using a StealthStation Treon image-guidance system (Medtronic) following standard practice. A Zeiss OPMI Pentero surgical microscope (Carl Zeiss Surgical GmbH) modified for fluorescence guidance with a 400-nm wavelength source for excitation and a 620–710-nm bandpass filter to record fluorescence emissions on a sensitive 3-chip charge-coupled device camera was also coregistered with the surgical field.

At various points during resection, the surgeon switched from white to blue light exposure to visualize fluorescence. Biopsy specimens were collected at the beginning, middle, and end of resection, as well as in fluorescing and nonfluorescing regions within the preoperatively planned resection volume, and were identified as corresponding to either the center or the edge of tumor. Biopsy specimens were separated into 3 equal parts for further processing as follows: one part was placed in formalin, another part was placed in optimal cutting temperature compound and frozen in liquid nitrogen, and the final part was placed in a cryogenic vial and frozen in liquid nitrogen. Briefly, immediately prior to biopsy acquisition, the surgeon placed the intraoperative probe on the location of the intended specimen and performed intraoperative probe recordings. Intraoperative probe data were recorded in less than 0.5 seconds and immediately converted into quantitative PpIX concentrations (that is, C_{PpIX}) in approximately 2 seconds. Control data were also acquired in each case consisting of spectroscopic measurements in normal brain (of indiscriminate subtypes) or normal dura mater.

Digital images were recorded under white and blue light for each biopsy acquisition, and the site was assigned a fluorescence score from 0 to 4 (0, no fluorescence; 1, minimal fluorescence; 2, moderate fluorescence; 3, high fluorescence; and 4, very high fluorescence) based on the impression of the surgeon (blinded to the quantitative measurement) of the visible fluorescence before the tissue was removed. Biopsy specimens were immediately separated into 3 equal parts for further processing. Resection was continued until the surgeon judged that no more malignant tissue that could be safely removed was present.

Histopathology

Histopathological analysis was performed on formalin-fixed paraffin embedded biopsy tissue specimens processed for H & E staining. A neuropathologist (B.T.H.) was blinded to the final pathological diagnoses in all cases. Each H & E–stained tissue section was assessed for the presence of tumor cells, necrosis, and reactive astrocytosis, and subsequently classified as normal or abnormal (tumor) tissue based on WHO histopathological criteria. Biopsy specimens were classified into 5 categories: normal tissue, LGG (WHO Grade I or II), HGG (WHO Grade III or IV), meningioma (WHO Grade I or II), and metastasis. A sixth diagnostic category, labeled “all tumors,” was introduced to group all abnormal biopsy specimens together for comparison with the normal control measurements.

Data Processing

Data processing was performed using MATLAB software (Version R2009b, The Mathworks, Inc.). The following 5 diagnostic variables were calculated to determine the diagnostic variable with the best classification efficiency: C_{PpIX}, A_{615}, A_{660}, P_{635}, and P_{710}. C_{PpIX} corresponds to the quantitative measurements of PpIX concentration derived from the light-transport modeling. A_{615} and A_{660} correspond to the total light intensity associated with the integration of the fluorescence emission spectrum from $\lambda = 615$ to 740 nm and from $\lambda = 660$ to 740 nm, respectively, whereas P_{635} and P_{710} refer to the peak intensities of the fluorescence emission spectrum at $\lambda = 635$ nm and $\lambda = 710$ nm, respectively.

Statistical Analysis

Statistical analyses were performed using Stata 10.1 software (Stata Corp.). Wilcoxon rank-sum (Mann-Whitney) tests were used to compare differences in fluorescence variables between tissue categories. We used ROC analysis to summarize the diagnostic performance of the fluorescence variables. The cutoff value with the best discriminative ability was chosen as the point on the curve closest to the upper left corner of the ROC graph.[15] Two-sided p values < 0.05 are described as statistically significant.

Results

The majority of work[6,12,13,16] using fluorescence spectroscopy as a tissue characterization tool (for example, in brain tumor studies) has been based on measurements of the raw emission spectrum without correcting for variations in tissue optical properties or the presence of other fluorophores. To assess the added value of our quantitative measurements, raw spectroscopic variables were also considered and their relative diagnostic performances were evaluated. Specifically, the variables A_{615}, A_{660}, P_{635}, and P_{710} were computed from the raw fluorescence emission spectrum.

Measurements were obtained under an institutional review board–approved protocol with informed consent during the open cranial surgeries in 14 patients with a range of tumor histologies: LGGs (in 2 patients), HGGs (in 3), meningiomas (in 6), and carcinoma of the lung metastases (in 3). In vivo spectra and corresponding tissue biopsies were recorded at distinct stages of the surgical procedure and were identified as corresponding to either the center or the edge of tumor in an effort to maximize the sampling extent of each lesion. Tissue samples from each biopsy site were also assessed histologically using H & E staining (Fig. 1). We found a statistically significant increase ($p < 0.05$) in C_{PpIX} across all of the tumor categories when compared with the normal controls. Figure 2 presents C_{PpIX} on a logarithmic scale for each tissue category, since the normal control values of C_{PpIX} can be up to 4 orders of magnitude smaller than in tumor. The other diagnostic variables—A_{615}, A_{660}, P_{635}, and P_{710}—did not show similar potential for discriminating between normal and abnormal intracranial tissue.

We used ROC analysis[15] to further assess the diagnostic performance of the fluorescence variables listed in Table 1. We found that C_{PpIX} stood out as the most accurate diagnostic variable based on an AUC metric. In fact, C_{PpIX} discriminated abnormal from normal tissue with a mean AUC of 0.95 ± 0.02 compared with mean AUCs of 0.54 ± 0.06, 0.54 ± 0.06, 0.60 ± 0.06, and 0.57 ± 0.06 (± SE) for A_{615}, A_{660}, P_{635} and P_{710}, respectively. As summarized in Table 2, ROC analysis of C_{PpIX} as a diagnostic biomarker resulted in classification efficiencies of 87% for all tumors, 76% for LGGs, 93% for HGGs, 97% for meningiomas, and 95% for the metastases group (Fig. 3B).

State-of-the-art clinical detection of PpIX during open cranial tumor resection is based on broad-beam blue light illumination and human visual perception and/or image capture (with a charge-coupled device) of the resulting fluorescence observed through the optics of the operating microscope. We have compared the sensitivity and specificity of this qualitative visual imaging approach with the quantitative fluorescence measurements presented here in the same cohort of patients (Fig. 3A). Specimens were assigned a fluorescence score from 0 to 4 (0, no fluorescence; 1, minimal fluorescence; 2, moderate fluorescence; 3, high fluorescence; and 4, very high fluorescence) based on the impression of the surgeon (blinded to the quantitative measurement) of the visible fluorescence before the tissue was removed. The optimal classification efficiency was 66% (specificity = 100%, sensitivity = 47%, PPV = 100%, NPV = 51%, cutoff value: fluorescence score = 1, that is, minimal level of observed fluorescence) when using the surgeon's visual assessment, compared with a classification efficiency of 87% (specificity = 92%, sensitivity = 84%, PPV = 95%, NPV = 77%, cutoff value: C_{PpIX}= 0.0074 μg/ml) when using the quantitative fluorescence measurements in the all tumors category. Furthermore, more than 81% (57 of 70) of the quantitative fluorescence measurements that were below the threshold of the surgeon's visual perception were classified correctly in an all-tumors analysis. Figure 3 shows ROC curves comparing the qualitative visual approach with the quantitative C_{PpIX} data, which is significantly more accurate (quantitative approach: AUC = 0.95 ± 0.02, visible approach: AUC = 0.73 ± 0.03; $p < 0.0001$).

Discussion

Here, we show that quantification of fluorescence signals measured intraoperatively and in vivo after accumulation of exogenously enhanced PpIX yields a highly specific and sensitive biomarker for intracranial tumors that holds promise as a diagnostic indicator for informing resection decisions during neurosurgery. Previous studies demonstrated that this biomarker accumulates with high specificity and in sufficient concentrations in HGG to allow visual fluorescence detection, and that this improves resection completeness and, concomitantly, disease-free survival.[9,18] However, current fluorescence imaging technologies (including the human visual system) do not take full advantage of the biological targeting of ALA-induced PpIX.[2,4,14,17,23] More specifically, we have shown that quantitative in vivo measurements based on a light-transport modeling approach, which corrects for the marked distorting effects of variations in tissue optical properties on the fluorescence emission spectrum and intensity, improve substantially the ROC performance of PpIX as a brain tumor diagnostic across a range of histologies.

Our work demonstrates that PpIX fluorescence is a more sensitive and specific biomarker for intracranial tumors than previously appreciated, thus promoting further work into understanding of the molecular basis of the cellular pathways involved in preferential ALA-induced PpIX accumulation in tumors per se. Importantly, the data presented here demonstrate that the biological targeting of ALA-induced PpIX fluorescence extends to LGGs with diagnostic fidelity, a finding that reverses current thinking that these tumors are not amenable to fluorescence-guided resection with this particular biomarker.[17, 23]

Currently, intraoperative tumor tissue detection relies on visual white light inspection, preoperative image guidance, intraoperative imaging[5] including qualitative observation of fluorescence,[4,14,18] and/or time-consuming, ex vivo diagnosis by a pathologist.[20] Here, we show the advantage of a light-transport modeling-based measurement approach compared with 4 direct but uncorrected spectroscopic metrics for intraoperative fluorescence-based tumor detection. Quantitative PpIX concentration (C_{PpIX}) yielded the best classification efficiency (87%) as a diagnostic variable for the category with all tumor histologies with a high specificity (that is, the probability of classifying tissue as normal tissue given that it is normal tissue) of 92%, a sensitivity (the probability of classifying tissue as abnormal tumor tissue given that it is abnormal tumor tissue) of 84%, a PPV (the probability that tissue is abnormal tumor tissue given that it is classified as abnormal tumor tissue) of 95%, and an NPV (the probability that tissue is normal given that it is classified as normal tissue) of 77%.[1,14] The derived specificity, sensitivity, NPV, and PPV are dependent on the chosen cutoff value. We have provided the cutoff values using a standard methodology for determining the optimal classification efficiency (Table 2).[15] One could increase the specificity at the cost of decreasing the sensitivity of our quantitative fluorescence approach by choosing a different cutoff value. Our quantitative approach also showed superior diagnostic detection of abnormal tissue in intracranial tumors compared with qualitative assessment of the visible fluorescence (classification efficiency: C_{PpIX} = 87% vs visible = 66%; AUC: C_{PpIX} = 0.95 vs visible = 0.73 [$p < 0.0001$]).

It is important to note that this study was performed only in individuals with a diagnosis of intracranial tumor. As a result, the prevalence of the disease under study (that is, the total number of abnormal tumor sites interrogated for analysis divided by the total number of both normal and abnormal sites interrogated) was high. Under certain assumptions (for example, a truly dichotomous disease status), sensitivity and specificity are independent of disease prevalence, whereas predictive values are highly dependent on disease prevalence.[1] The purpose of this study was to demonstrate that our quantitative approach, when compared with the subjective approach in ALA-induced PpIX fluorescence-guided resection, provides more accurate tumor tissue identification. Since this technique is intended for use in patients with a presumed preoperative diagnosis of intracranial tumor using conventional neurosurgical technique (for example, MR image guidance), prevalence of the disease will always be high, and as such, predictive values would be expected to remain within a diagnostically acceptable, high range. We are currently enrolling more patients to validate the results of our quantitative approach.

Conclusions

We believe that this quantitative approach for intraoperative in vivo measurement of PpIX concentrations opens the door to real-time delineation and diagnosis of intracranial tumor histologies beyond HGGs.[10,14,17,18,23] We have used this approach as an adjuvant to standard white-light and qualitative fluorescence image-guided resection in the first demonstration of truly quantitative surgical guidance. Furthermore, if the concentration of PpIX can be quantitatively imaged over the entire resection cavity during surgery, the approach is likely to increase not only the completeness of resection but also the frequency with which complete resections can be safely achieved in tumor surgeries, including those for LGGs, where the impact on patient survival could be substantial.[11]

Acknowledgments

This study was supported by National Institutes of Health Grant Nos. R01NS052274-01A2 (D.W.R.) and K25CA138578 awarded by the National Cancer Institute (F.L.). The authors acknowledge the support of Medtronic Navigation (Medtronic) and Carl Zeiss (Carl Zeiss Surgical GmbH) for use of the StealthStation Treon navigation system and the OPMI Pentero operating microscope, respectively. They also acknowledge DUSA Pharmaceuticals

for their supplying of ALA. Drs. Kim and Wilson have a provisional patent (61,297,969) for the device under study.

Appendix

A handheld probe developed for fluorescence and white light reflectance measurements was used intraoperatively.[7] Briefly, 4 optical fibers, each with a 200-μm diameter core spaced (linearly) 260 μm apart, were bundled into an 18-gauge stainless steel shaft forming the tissue-contact end of the probe. The fibers were connected to the data acquisition system through a 3-m cable. White light reflectance and fluorescence emission spectra were collected during each measurement following sequential white light (wavelength range 450–720 nm) and fluorescence excitation light (at 405 nm) exposure through the fiberoptics, with 1 fiber connected to a spectrometer onboard the data acquisition system.

The absolute concentration of PpIX (C_{PpIX}) was calculated using a light-transport model, which extracted the quantitative fluorescence spectrum from the intraoperative recordings. The tissue optical properties (that is, absorption and reduced-scattering coefficients) were estimated from the white light reflectance to correct for their distorting effects on the fluorescence emission signal by minimizing the error between probe measurements and a spectrally constrained model of the diffuse reflectance in a Levenberg-Marquardt algorithm. The resulting quantitative (and corrected) fluorescence spectrum was estimated from the model and used to determine biomarker (that is, PpIX) concentration through a fluorescence basis spectrum equivalent to unit concentration (μg/ml).

Briefly, the fluorescence model assumed that 1) absorption at the excitation wavelength is much larger than absorption at the fluorescence emission wavelengths (that is, $\mu_{a,x} \gg \mu_{a,m}$ where excitation and emission wavelengths are denoted by the subscripts x and m, respectively) because the fluorescent biomarker's contribution to $\mu_{a,x}$ is small when compared with the high absorption of hemoglobin in the range 380–450 nm; and 2) fluorescence and reflectance photons travel similar path lengths given the same fiberoptic distance (and $\mu_{a,x} \gg \mu_{a,m}$). Under these assumptions, the measured fluorescence, $F_{x,m}$, has a linear relationship with reflectance at the emission wavelength, R_m: $F_{x,m} = SR_m$, where S represents the fraction of photons reemitted as fluorescence, which is a function not only of the fluorophore concentration but also the tissue optical properties at the excitation wavelength.

The quantitative fluorescence spectrum was extracted from the spectrally constrained model, yielding an emission spectrum, f, with the distorting effects of variations in optical properties removed. This corrected fluorescence emission spectrum was used to quantify biomarker (that is, PpIX) concentration, c, through a fluorescence basis spectrum, b, equivalent to unit concentration (μg/ml) from the relation, f = bc, where f and b are column vectors and c is computed by pseudoinversion as $c = (b^T b)^{-1} b^T f$.

Generalization to N fluorescent biomarkers, each with different spectra, is possible by forming a basis matrix, $B = [b_1\ b_2\ \ldots\ b_N]$, composed of the individual basis spectra for each fluorescent biomarker, and calculating biomarker concentrations, $c = [c_1\ c_2\ \ldots\ c_N]^T$.

References

1. Brenner H, Gefeller O. Variation of sensitivity, specificity, likelihood ratios and predictive values with disease prevalence. Stat Med. 1997; 16:981–991. [PubMed: 9160493]
2. Collaud S, Juzeniene A, Moan J, Lange N. On the selectivity of 5-aminolevulinic acid-induced protoporphyrin IX formation. Curr Med Chem Anticancer Agents. 2004; 4:301–316. [PubMed: 15134506]

3. Dysart JS, Patterson MS. Photobleaching kinetics, photoproduct formation, and dose estimation during ALA induced PpIX PDT of MLL cells under well oxygenated and hypoxic conditions. Photochem Photobiol Sci. 2006; 5:73–81. [PubMed: 16395430]
4. Floeth FW, Stummer W. The value of metabolic imaging in diagnosis and resection of cerebral gliomas. Nat Clin Pract Neurol. 2005; 1:62–63. [PubMed: 16932494]
5. Galloway RL Jr. The process and development of image-guided procedures. Annu Rev Biomed Eng. 2001; 3:83–108. [PubMed: 11447058]
6. Haj-Hosseini N, Richter J, Andersson-Engels S, Wårdell K. Optical touch pointer for fluorescence guided glioblastoma resection using 5-aminolevulinic acid. Lasers Surg Med. 2010; 42:9–14. [PubMed: 20077492]
7. Kim A, Khurana M, Moriyama Y, Wilson BC. Quantification of in vivo fluorescence decoupled from the effects of tissue optical properties using fiber-optic spectroscopy measurements. J Biomed Opt. 2010; 15:067006. [PubMed: 21198210]
8. Nabavi A, Thurm H, Zountsas B, Pietsch T, Lanfermann H, Pichlmeier U, et al. Five-aminolevulinic acid for fluorescence-guided resection of recurrent malignant gliomas: a phase ii study. Neurosurgery. 2009; 65:1070–1077. [PubMed: 19934966]
9. Pichlmeier U, Bink A, Schackert G, Stummer W. Resection and survival in glioblastoma multiforme: an RTOG recursive partitioning analysis of ALA study patients. Neuro Oncol. 2008; 10:1025–1034. [PubMed: 18667747]
10. Pogue BW, Gibbs-Strauss SL, Valdes PA, Samkoe KS, Roberts DW, Paulsen KD. Review of neurosurgical fluorescence imaging methodologies. IEEE J Sel Top Quantum Electron. 2010; 16:493–505. [PubMed: 20671936]
11. Pouratian N, Asthagiri A, Jagannathan J, Shaffrey ME, Schiff D. Surgery insight: the role of surgery in the management of low-grade gliomas. Nat Clin Pract Neurol. 2007; 3:628–639. [PubMed: 17982433]
12. Ramanujam N. Fluorescence spectroscopy of neoplastic and non-neoplastic tissues. Neoplasia. 2000; 2:89–117. [PubMed: 10933071]
13. Richards-Kortum R, Sevick-Muraca E. Quantitative optical spectroscopy for tissue diagnosis. Annu Rev Phys Chem. 1996; 47:555–606. [PubMed: 8930102]
14. Roberts DW, Valdes PA, Harris BT, Fontaine KM, Hartov A, Fan X, et al. Coregistered fluorescence-enhanced tumor resection of malignant glioma: relationships between δ-aminolevulinic acid-induced protoporphyrin IX fluorescence, magnetic resonance imaging enhancement, and neuropathological parameters. Clinical article. J Neurosurg. 2011; 114:595–603. [PubMed: 20380535]
15. Shapiro DE. The interpretation of diagnostic tests. Stat Methods Med Res. 1999; 8:113–134. [PubMed: 10501649]
16. Sokolov K, Follen M, Richards-Kortum R. Optical spectroscopy for detection of neoplasia. Curr Opin Chem Biol. 2002; 6:651–658. [PubMed: 12413550]
17. Stummer W, Novotny A, Stepp H, Goetz C, Bise K, Reulen HJ. Fluorescence-guided resection of glioblastoma multiforme by using 5-aminolevulinic acid-induced porphyrins: a prospective study in 52 consecutive patients. J Neurosurg. 2000; 93:1003–1013. [PubMed: 11117842]
18. Stummer W, Pichlmeier U, Meinel T, Wiestler OD, Zanella F, Reulen HJ. Fluorescence-guided surgery with 5-aminolevulinic acid for resection of malignant glioma: a randomised controlled multicentre phase III trial. Lancet Oncol. 2006; 7:392–401. [PubMed: 16648043]
19. Stummer W, Reulen HJ, Meinel T, Pichlmeier U, Schumacher W, Tonn JC, et al. Extent of resection and survival in glioblastoma multiforme: identification of and adjustment for bias. Neurosurgery. 2008; 62:564–576. [PubMed: 18425006]
20. Uematsu Y, Owai Y, Okita R, Tanaka Y, Itakura T. The usefulness and problem of intraoperative rapid diagnosis in surgical neuropathology. Brain Tumor Pathol. 2007; 24:47–52. [PubMed: 18095130]
21. Valdés PA, Fan X, Ji S, Harris BT, Paulsen KD, Roberts DW. Estimation of brain deformation for volumetric image updating in protoporphyrin IX fluorescence-guided resection. Stereotact Funct Neurosurg. 2010; 88:1–10. [PubMed: 19907205]

22. Weissleder R, Pittet MJ. Imaging in the era of molecular oncology. Nature. 2008; 452:580–589. [PubMed: 18385732]
23. Widhalm G, Wolfsberger S, Minchev G, Woehrer A, Krssak M, Czech T, et al. 5-Aminolevulinic acid is a promising marker for detection of anaplastic foci in diffusely infiltrating gliomas with nonsignificant contrast enhancement. Cancer. 2010; 116:1545–1552. [PubMed: 20108311]

Abbreviations used in this paper

ALA	δ-aminolevulinic acid
AUC	area under the curve
A_{615}	total light intensity associated with the integration of the fluorescence emission spectrum from λ = 615 to 740 nm
A_{660}	total light intensity associated with the integration of the fluorescence emission spectrum from λ = 660 to 740 nm
C_{PpIX}	absolute concentration of PpIX
HGG	high-grade glioma
LGG	low-grade glioma
NPV	negative predictive value
PpIX	protoporphyrin IX
PPV	positive predictive value
P_{635}	peak intensity of the fluorescence emission spectrum at λ = 635 nm
P_{710}	peak intensity of the fluorescence emission spectrum at λ = 710 nm
ROC	receiver operating characteristic

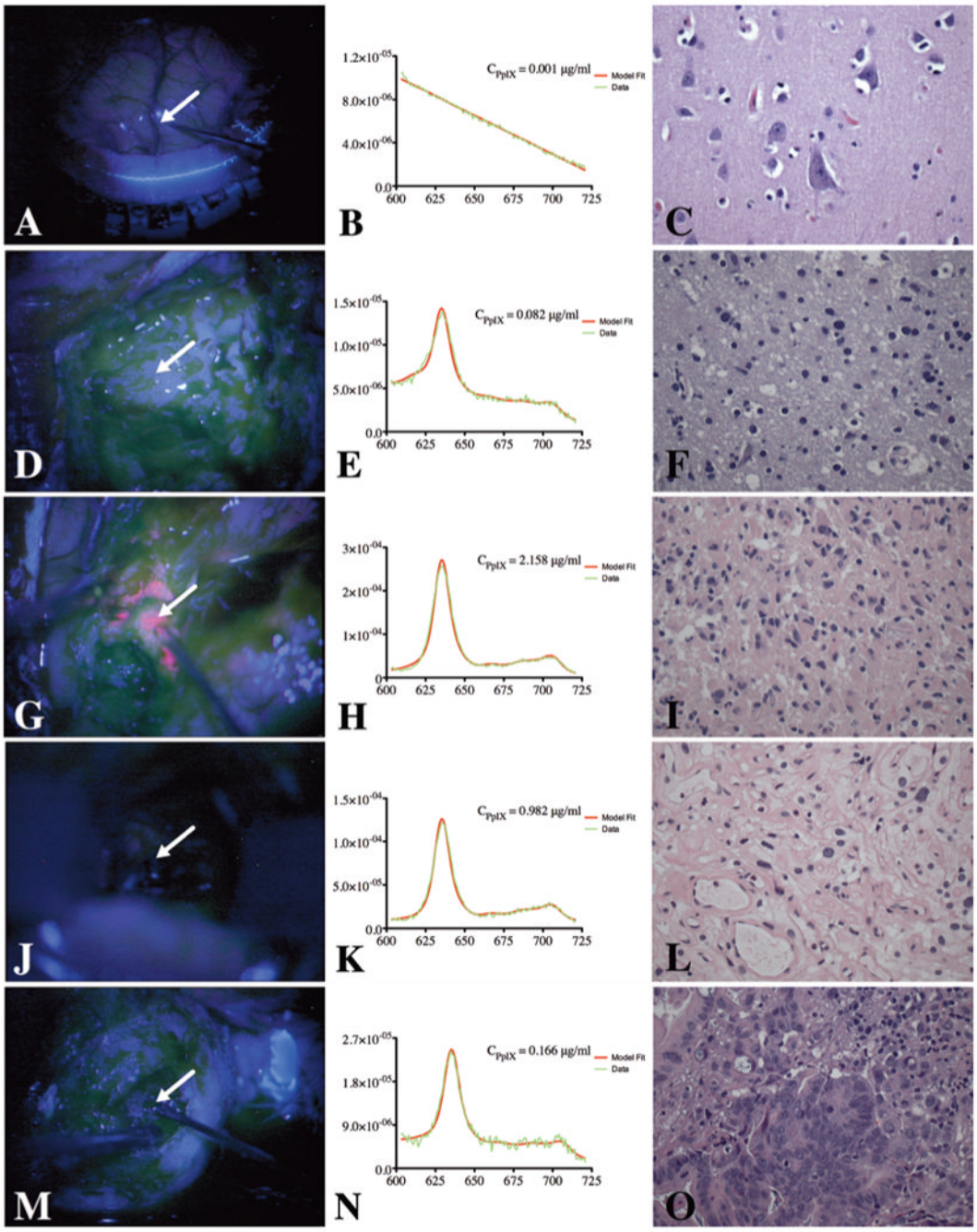

Fig. 1.

In vivo spectroscopic measurements of ALA-induced PpIX fluorescence during intracranial tumor resection surgeries. **Left:** Intraoperative fluorescence images of the resection cavity visible to the surgeon through the operating microscope under blue light exposure. The *arrows* indicate the location of the handheld probe tip where the spectroscopic measurements and tissue specimens were acquired. **Center:** Raw fluorescence spectra (data, *green*) and modeled quantitative in vivo fluorescence spectra (model fit, *red*) measured at each interrogated site (the characteristic spectral features of PpIX, that is, emission peaks at λ = 635 nm and λ = 710 nm, are evident). The units for the values on the y axis are

$nm^{-1}cm^{-1}$ and those for the values on the x axis are nm. **Right:** Histological tissue sections of the specimens (H & E, original magnification × 40). The rows correspond to normal cortex **(A–C)**, LGG **(D–F)**, HGG **(G–I)**, meningioma **(J–L)**, and metastasis **(M–O)**. The HGG displays visible levels of fluorescence while the LGG, meningioma, and metastasis exhibit no visible fluorescence; all of the tumor histologies have measurable C_{PpIX} relative to normal cortex, whose spectrum is devoid of the characteristic signal features of PpIX and its associated photoproducts.

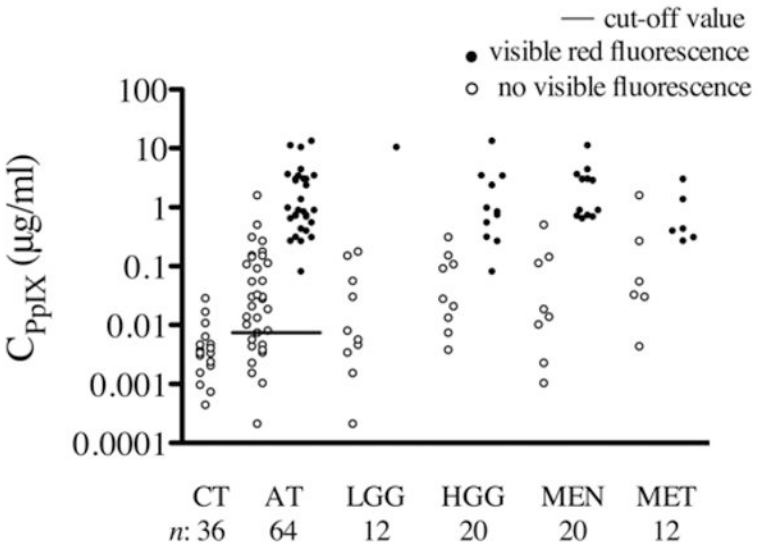

Fig. 2.

Concentration of ALA-induced PpIX, C_{PpIX}. *Circles* represent the C_{PpIX} value calculated in vivo using the light-transport model for each location where measurements were collected, with *filled circles* representing interrogated sites with visible red fluorescence, and *open circles* representing interrogated sites with no visible fluorescence. The cutoff value is determined from the quantitative probe measurements, and n represents the number of locations measured for controls (CT), all tumors combined (AT), and the 4 tumor categories: LGG, HGG, meningioma (MEN), and metastasis (MET). The y axis is logarithmic. Statistically significant differences in C_{PpIX} were found between normal and abnormal intracranial tissue: all tumors ($p < 0.0001$), LGGs ($p < 0.05$), HGGs ($p < 0.0001$), meningiomas ($p < 0.0001$), and metastases ($p < 0.001$).

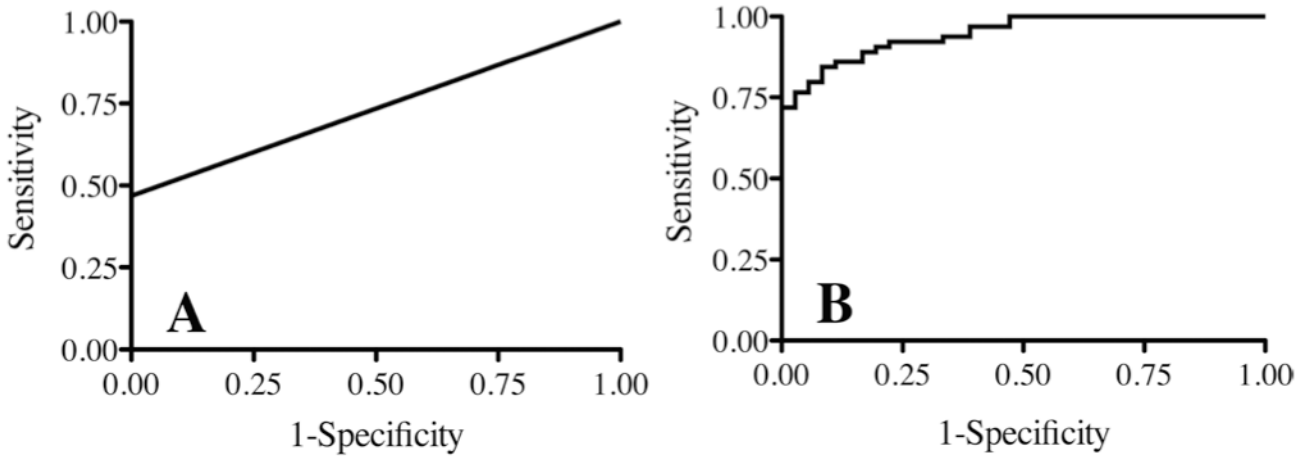

Fig. 3.

The ROC curve analysis of intraoperative detection of ALA-induced PpIX. **A:** Curve for all tumors using visible in vivo fluorescence as a diagnostic variable (AUC = 0.73 ± 0.03). **B:** Curve for all tumors using quantitative in vivo PpIX concentration, C_{PpIX}, as a diagnostic variable (AUC = 0.95 ± 0.02).

TABLE 1

Receiver operating characteristic curve analysis of each diagnostic variable in the 5 categories of pathogenic tissues*

	AUC					
Group	**Vis**	**C_{PpIX}**	**A_{615}**	**A_{660}**	**P_{635}**	**P_{710}**
AT	0.73 ± 0.03	0.95 ± 0.02	0.54 ± 0.06	0.54 ± 0.06	0.60 ± 0.06	0.57 ± 0.06
LGG	0.54 ± 0.04	0.75 ± 0.12	0.20 ± 0.11	0.18 ± 0.11	0.32 ± 0.14	0.17 ± 0.11
HGG	0.78 ± 0.06	0.96 ± 0.03	0.54 ± 0.11	0.54 ± 0.11	0.65 ± 0.11	0.61 ± 0.11
MEN	0.80 ± 0.06	0.99 ± 0.02	0.70 ± 0.09	0.70 ± 0.09	0.73 ± 0.09	0.73 ± 0.09
MET	0.75 ± 0.08	0.98 ± 0.02	0.63 ± 0.14	0.59 ± 0.15	0.67 ± 0.14	0.67 ± 0.14

*Data are presented as the means ± SEs. Abbreviations: AT = all tumors; MEN = meningioma; MET = metastasis; Vis = qualitative visual imaging.

TABLE 2

Summary of ROC analysis of C_{PpIX} as a diagnostic variable*

Group	CO (μg/ml)	Classification Efficiency (%)	ROC AUC	Sn (%)	NPV (%)	Sp (%)	PPV (%)
AT	0.0074	87	0.95	84	77	92	95
LGG	0.0034	76	0.75	75	57	80	90
HGG	0.0074	93	0.96	95	89	89	89
MEN	0.0010	97	0.98	100	100	93	95
MET	0.0302	95	0.97	92	89	100	100

*C_{PpIX} threshold values (in μg/ml) with corresponding classification efficiencies, AUCs, sensitivities (Sn), and specificities (Sp), for abnormal tumor tissue are tabulated. Abbreviation: CO = cutoff value.

J Neurosurg. Author manuscript; available in PMC 2012 July 01.